



Optimization of an enriched mixed culture to increase PHA accumulation using industrial saline complex wastewater as a substrate

Lucía Argiz, Andrea Fra-Vázquez, Ángeles Val del Río, Anuska Mosquera-Corral

Accepted Manuscript

How to cite:

Chemosphere, Volume 247, May 2020, 125873

Doi: 10.1016/j.chemosphere.2020.125873

Copyright information:

© 2020 Elsevier Ltd. This manuscript version is made available under the CC-BY-NC-ND 4.0 license (<http://creativecommons.org/licenses/by-nc-nd/4.0>)

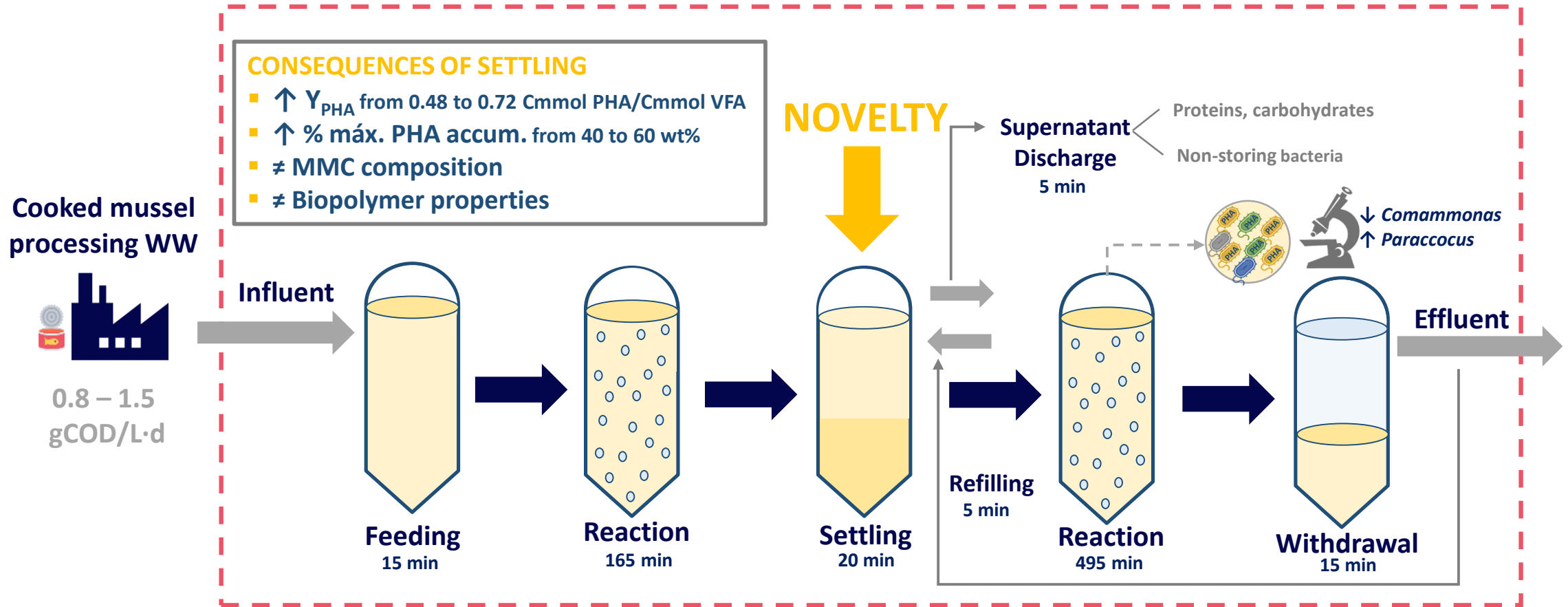
Optimization of an enriched mixed culture to increase PHA accumulation using industrial saline complex wastewater as a substrate

Lucia Argiz*, Andrea Fra-Vazquez, Angeles Val del Rio and Anuska Mosquera-Corral

School of Engineering, Department of Chemical Engineering, Universidade de Santiago de Compostela, 15782 Santiago de Compostela, Galicia, Spain.

* Corresponding author. Tel.: +34 881816784. E-mail address: luciaargiz.montes@usc.es

Polyhydroxyalkanoates (PHA) production – Enrichment stage



Highlights

- Complex saline industrial wastewater as a substrate for PHA production.
- A settling stage was included in the enrichment cycle after VFA consumption.
- Proteins and carbohydrates promoting growth instead of PHA production were removed.
- The PHA production yield increased from 0.48 to 0.72 $\text{Cmmol}_{\text{PHA}} / \text{Cmmol}_{\text{VFA}}$.
- The maximum PHA storage capacity of the MMC improved from 40 to 60 wt%.

1 **Optimization of an enriched mixed culture to increase PHA**
2 **accumulation using industrial saline complex wastewater as a**
3 **substrate**

4 Lucia Argiz*, Andrea Fra-Vazquez, Angeles Val del Rio and Anuska Mosquera-Corral

5 School of Engineering, Department of Chemical Engineering, Universidade de Santiago de
6 Compostela, 15782 Santiago de Compostela, Galicia, Spain.

7 * Corresponding author. Tel.: +34 881816784. E-mail address: luciaargiz.montes@usc.es

8

9 **ABSTRACT**

10 Polyhydroxyalkanoates (PHA) appear as good candidates to substitute conventional petroleum-based
11 plastics since they have similar properties but with the advantage of being biodegradable. Wastewater
12 streams with high organic content are feasible substrates for PHA production resulting in an opportunity
13 for waste recovery. One of the main challenges is the optimization of the selection of microorganisms
14 with high PHA storage capacity. This microbial selection is performed in sequencing batch reactors
15 (SBR) operated under an aerobic feast/famine (F/F) regime. In the present study, a settling stage was
16 added at the end of the feast phase of the enrichment cycle of a SBR fed with pre-acidified cooked mussel
17 processing wastewater (containing up to 12 g NaCl/L). Settling and subsequent supernatant discharge
18 favoured the wash-out of non-accumulating microorganisms as well as the removal of substances that
19 enhanced their undesired development (proteins and carbohydrates). Microbial analysis performed by
20 fluorescence *in situ* hybridization (FISH) technique showed shifts in the microbial community; the
21 presence of genus *Paracoccus* increased whereas genera *Comamonas* decreased. Moreover, the process
22 efficiency was improved with the increase of the PHA production yield (Y_{PHA}) and the maximum PHA
23 storage capacity (max. PHA) from 0.48 to 0.72 Cmmol_{PHA} / Cmmol_{VFA} and from 40 to 60 wt%,
24 respectively. The polymer composition also changed, its HB:HV ratio varied from 83:17 to 70:30. Results
25 obtained in the present study showed that settling promoted the removal of carbon sources that did not
26 contribute to PHA production and the washout of non-storing bacteria, which favoured the culture
27 enrichment.

28

29 **Keywords:** bioplastics; enrichment; industrial wastewater, mixed microbial culture;
30 polyhydroxyalkanoates; valorization.

31

32

33

34 **1. INTRODUCTION**

35 Plastics are polymers that are present in nearly all aspects of modern life. The great
36 majority are petroleum-based products, durable in use but no biodegradable (Zhu et al.,
37 2013). This fact, in addition to petroleum depletion, has derived in a growing interest in
38 the development of more sustainable alternatives. Polyhydroxyalkanoates (PHA) are a
39 family of biobased, biodegradable and biocompatible linear polyesters (Keshavarz and
40 Roy, 2010) that have been recognized as good candidates to substitute conventional
41 plastics due to their similar properties (Dias et al., 2006). These polymers are produced
42 by certain microorganisms and accumulated as intracellular carbon sources under stress
43 conditions (Reddy et al., 2003). Nowadays, large scale PHA production is based on the
44 use of pure cultures or genetically modified microorganisms that require sterile
45 conditions and highly costly specific substrates (Jiang et al., 2016). Consequently, PHA
46 are not yet competitive in bulk materials markets (Albuquerque et al., 2010). Its current
47 price ranges from 2.2 – 5.0 €/kg, which is more than one-third of the cost reported from
48 the beginning of the last decade but still high in comparison to petroleum-based
49 polymers, which typically cost less than 1.0 €/kg (Valentino et al., 2017). In recent
50 years, research has been focused on the development of cost-effective processes, which
51 involve the use of low-value substrates and mixed microbial cultures that do not need
52 sterile conditions (Albuquerque et al., 2011) and allow the production of high quality
53 biopolymers with a purity (> 98 %) comparable to those obtained using pure cultures
54 (Samorì et al., 2015).

55 Wastewater streams produced in the agro-alimentary sector are among the most suitable
56 substrates for PHA production due to their high organic matter content (Nikodinovic-
57 Runic et al., 2013). This is the case of fish-canning industries, which generate large
58 volumes of effluents with high pollutant load. In this way, wastewater valorization for

59 PHA production contributes to the transition to a circular economy model: on one hand,
60 organic matter is recovered and converted into resources and on the other hand,
61 pollutants are removed and treated wastewater can be discharged to natural water
62 bodies. In this way, the concept of wastewater treatment plant (WWTP) moves to a
63 water resource recovery facility (WRRF).

64 The PHA production system with a mixed microbial culture (MMC) using industrial
65 wastewater as substrate generally consists on a three-stage process: (1) substrate pre-
66 acidification (if necessary) to obtain a suitable carbon source for PHA production,
67 primarily volatile fatty acids (VFA); (2) selection and enrichment of the MMC in PHA-
68 accumulating organisms; and (3) maximization of the PHA storage before biopolymer
69 extraction and purification. The main challenge of this PHA production system is the
70 selection of a MMC with high PHA-storage capacity (Albuquerque et al., 2010). One of
71 the most common strategies to achieve the microbial enrichment is the application of
72 cycles of presence/absence of substrate known as feast/famine regime (F/F) or aerobic
73 dynamic feeding (ADF), operated in sequencing batch reactors (SBR) (Albuquerque et
74 al., 2007). In the last decade, research has been focused on the development of new
75 strategies for the optimization of the culture enrichment. It has been implemented
76 variations such as nitrogen limitation in the feast phase and/or the integration of an
77 intermediate settling phase in the SBR cycle (Kourmentza et al., 2017).

78 Nitrogen deficiency during the feast phase restricts the growth of non-PHA
79 accumulating bacteria while providing nitrogen during the famine enables their growth,
80 which allows faster selection of a more efficient PHA-storing culture (Ahmadi et al.,
81 2018; Oliveira et al., 2017). For example, Marang et al. (2014) observed that the
82 presence of methanol and acetate promoted the development of non-accumulating
83 microorganisms in the MMC. To solve this problem, Korkakaki et al. (2016) proposed

84 the addition of a settling phase after the acetate depletion in order to eliminate the
85 methanol with the supernatant and promote the enrichment of the MMC by limiting the
86 growth of non-accumulating bacteria. As a result, they observed a considerable increase
87 in the maximum PHA storage capacity of the biomass from 48 wt% to 70 wt%.
88 Supernatant discharge just after acetate depletion avoided the consumption of the
89 remaining organic matter (methanol) and the consequent growth of side-populations
90 increasing the proportion of PHA-producers in the mixed culture (Kourmentza et al.,
91 2017). Therefore, this modification of the SBR enrichment cycle can be considered as a
92 good solution to improve the microbial selection when there is more than one carbon
93 source in the substrate. However, until now few studies have explored this alternative
94 with industrial complex wastewater.

95 The objective of the present study was to improve the selection of PHA-accumulating
96 bacteria in a MMC using pre-acidified cooked mussel processing wastewater (with 4 -
97 12 g NaCl/L and high VFA content) as feedstock. To achieve this goal, a settling stage
98 was implemented in the operational cycle of an enrichment SBR working under F/F
99 regime with the aim of removing undesired substances (mainly proteins and
100 carbohydrates) that promoted the growth of non-accumulating bacteria. The enrichment
101 of the system was evaluated in terms of maximum PHA production and shifts in the
102 microbial community comprising the mixed culture.

103 **2. MATERIALS AND METHODS**

104 **2.1 Experimental set-up**

105 For the optimization of the enrichment unit and the consequent evaluation of maximum
106 PHA accumulation of the system, two lab-scale reactors were operated: an enrichment
107 reactor (SBR type) and an accumulation fed-batch reactor (FBR), respectively.

108 **2.1.1 Enrichment SBR for culture selection**

109 A tubular glass SBR with a working volume of 2 L (SBR-S) was inoculated with PHA-
110 accumulating enriched biomass (0.80 g VSS/L) adapted to saline conditions from other
111 SBR (SBR-I). The SBR-I was operated under the F/F regime treating pre-acidified
112 wastewater collected from a cooked mussel processing industry. This reactor operated
113 in cycles of 12 hours consisting of 15 min of feeding, 690 min of aerobic reaction and
114 15 min of effluent withdrawal and was completely aerated (Figure S1.A of
115 Supplementary Material). The SBR-S operation was modified with respect to SBR-I by
116 means of including a settling stage at the end of the feast phase. Therefore, the
117 operational cycles of the SBR-S comprised the following stages: 1) 0.8 L of feeding (15
118 min), 2) aerobic reaction (165 min), 3) settling (20 min), 4) 1 L of supernatant
119 discharge (5 min), 5) reactor refilling with 0.8 L of the previous cycle effluent
120 (recirculation) and 0.2 L of tap water (5 min), 6) aerobic reaction, (495 min) and 7) 0.8
121 L of effluent withdrawal, (15 min). Specific details about the cycle distribution can be
122 consulted in the Figure S1. B.

123 Aeration was supplied during all stages, except for settling and supernatant discharge,
124 through a diffuser located at the bottom of the reactor that granted the complete mixture
125 of the system. The temperature was controlled at 30 °C by a thermostatic bath (Techne
126 Inc., USA) and the pH was not controlled but periodically measured at the end of the
127 famine phase. A detailed scheme of the SBR-S can be seen in Figure S2 of
128 Supplementary Material.

129 The length of the aerobic reaction before the settling phase was established by the
130 duration of the feast phase, and stopped when the VFA had just been depleted
131 (Korkakaki et al., 2016). Since during the operation of the SBR-I, reactor where the
132 inoculum was obtained, the feast phase lasted from 2.5 to 3.0 h, the settling stage in the

133 SBR-S was imposed after 2.75 h (165 min) of aerobic reaction. In addition, to enable
134 the maintenance of a comparable hydraulic and sludge retention time (HRT and SRT,
135 respectively) of 24 h, and ensure biomass duplication (Korkakaki et al., 2016), the
136 effluent volume was established at 0.8 L.

137 The influent consisted of centrifuged pre-acidified cooked mussel processing
138 wastewater that was five-times diluted with tap water. It was supplemented with an
139 amount of 1.5 mL/L of 33.0 g/L allylthiourea (ATU) solution to inhibit the nitrification
140 activity, and 0.25 mL/L of antifoam agent (Y-30 Emulsion, Sigma Aldrich) to avoid
141 problems of foam during aerated phases. The organic loading rate (OLR) varied
142 between 0.8 and 1.5 g COD/(L·d). The pH of the influent was 6.5 ± 0.5 and its total
143 nitrogen (TN), dissolved organic carbon (DOC) and soluble chemical oxygen demand
144 (CODs) concentrations were 0.14 – 0.31 g /L, 0.41 – 0.93 g /L and 0.97 – 1.86 g /L,
145 respectively. The organic fraction mainly contained VFA (47.45 – 61.15 % g COD_{VFA}/g
146 sCOD) and proteins (34.08 – 39.58 % g COD_{proteins}/g sCOD), and to a lesser extent,
147 carbohydrates (2.10 – 4.45 % g COD_{carbohydrates}/g sCOD). In addition, this wastewater
148 was characterized by high NaCl concentrations (4.34 – 12.10 g/L). Variations observed
149 in the composition of the influent are a consequence of changes in the factory process.

150 The characteristics of the SBR-S influent, the supernatant discharged after settling, and
151 the effluent were analysed weekly (typically from two to three days) during the
152 complete operational period (70 days). Additionally, two enrichment operational cycles
153 (days 24 and 62) were monitored. Several parameters were determined in both cases:
154 dissolved oxygen (DO), pH, solids, organic matter constituents, nitrogen species and
155 salinity. PHA content was also analysed during the complete monitoring of the
156 enrichment cycles.

157

158 **2.1.2 Accumulation FBR experiments to determine maximum PHA accumulation**
159 **capacity**

160 Two accumulation assays were carried out in a 2.0 L FBR with biomass collected from
161 the SBR-S (days 35 and 64 of operation) in order to evaluate the maximum storage
162 capacity of the MMC. The system was continuously aerated a completely mixed by
163 means of a diffuser located at the bottom of the reactor. The temperature was controlled
164 at 30 °C by a thermostatic bath (Techne Inc., USA) and the pH was not controlled. A
165 detailed scheme of the FBR operation can be seen in Figure S3 (Supplementary
166 Material).

167 To maximize PHA accumulation, the FBR was operated under complete aeration and
168 excess of organic carbon. Bacterial growth was prevented by the absence of nutrients in
169 the influent. The carbon source was added in pulses of 50 mL with a content of 30
170 Cmmol of a mixture of VFA mimicking the pre-acidified cooked mussel wastewater
171 composition (11.42 g/L of acetic, 2.76 g/L of propionic, 2.48 g/L of butyric and 0.24
172 g/L of valeric acids). Pulses were added once the carbon compounds fed in the previous
173 pulse were consumed, which was indicated by changes in the DO concentration profile.
174 The maximum accumulation capacity was reached once the DO concentration remained
175 at saturation values, even after the addition of a substrate pulse.

176 **2.2 Analytical methods**

177 The DO concentration and the temperature were monitored on-line with a probe (model
178 HQ40d, Hach-Lange, USA), and the pH was measured with a pH & Ion-Meter (model
179 GLP 22, Crison, Spain).

180 Total and Volatile Suspended Solids (TSS and VSS, respectively) and total COD
181 (tCOD) were analyzed in raw samples according to Standard Methods for the

182 Examination of Water and Wastewater (APHA-AWA-WEF, 2017). Filtered liquid
183 samples (0.45 μm pore size, cellulose-ester membrane, Advantec, Japan) were taken for
184 the determination of: soluble COD (sCOD), VFA, carbohydrates, proteins, DOC, total
185 nitrogen (TN), ammonium (NH_4^+) and other ions (Na, Cl $^-$). sCOD was determined by
186 the open reflux method (APHA-AWWA-WEF, 2017). VFA were determined in a gas
187 chromatograph (Hewlett Packard 5890A, USA) equipped with a flame ionization
188 detector (FID) and an automatic injector (Hewlett Packard 7673A, USA).
189 Carbohydrates were measured by the Loewus method (Loewus, 1952) and expressed in
190 equivalent glucose (Glu) (balances were performed considering that 1 g of Glu contains
191 1.07 g of COD). Proteins were analyzed by the Lowry method (Lowry et al., 1951) and
192 expressed in equivalent bovine serum albumin (BSA) (balances were calculated taking
193 into account that 1 g of BSA contains 1.32 g of COD and 0.15 g of N). DOC and TN
194 were measured by catalytic combustion in the TOC-L CNS analyzer with the TNM-1
195 module (Shimadzu, Japan). NH_4^+ was determined by the Bower/Holm Hansen method
196 (Bower and Holm-Hansen, 1980) and ions by ion chromatography (861 Advanced
197 Compact IC, Metrohm, Switzerland).

198 PHA analysis was performed in the solid phase. For that purpose, fresh biomass
199 samples were centrifuged, frozen and freeze-dried. The PHA content (as g PHA/g VSS)
200 was measured following the method described by Smolders et al., (1994) for the
201 quantification of the monomer propyl esters present in a lyophilized sample. A
202 commercial PHA standard (Sigma-Aldrich, USA) containing 88 % of hydroxybutyrate
203 (HB) and 12 % of hydroxyvalerate (HV) and benzoic acid as internal standard was used.
204 The propyl esters were analyzed by means of gas chromatography in a HP innovax
205 column equipped with a FID (Agilent, USA).

206

2072.3 Calculations

208 Carbon and nitrogen balances were calculated to evaluate the effects of settling
209 implementation and effluent recirculation for the replacement of the supernatant
210 discharge.

211 The PHA content of the biomass samples was determined on a mass basis and
212 expressed in dry weight (wt%) as a percentage of the measured VSS (g VSS), according
213 to Eq. 1.

$$214 \quad PHA \text{ (wt\%)} = g \text{ PHA} / g \text{ VSS} \times 100 \quad Eq. 1$$

215 The elemental composition of the active biomass (X) was assumed to be $CH_{1.8}O_{0.5}N_{0.2}$
216 and its amount (as $Cmmol_X$) was determined by the subtraction of the accumulated
217 PHA from the mass of VSS.

218 Maximum specific conversion rates of VFA consumption (q_{VFA} ,
219 $Cmmol_{VFA}/(Cmmol_X \cdot h)$) and PHA production (q_{PHA} , $Cmmol_{VFA}/(Cmmol_X \cdot h)$) (for both
220 HB and HV) were determined from the maximum slopes of the curves obtained from
221 the corresponding experimental data, divided by the active biomass. Yields for HB
222 (Y_{HB}), HV (Y_{HV}) and biomass growth (Y_X) were obtained dividing the production rate
223 ($Cmmol_{PHA}/h$ and $Cmmol_X/h$) by the VFA consumption rate ($Cmmol_{VFA}/h$). HB:HV
224 ratio was calculated as the amount of each compound ($Cmmol_{HB}$ or $Cmmol_{HV}$) divided
225 by the total amount of PHA ($Cmmol_{PHA}$).

226 2.4 Identification of microbial populations

227 For the identification of the different populations of the enriched MMC, biomass
228 samples were analyzed by the fluorescence *in situ* hybridization (FISH) following the
229 procedure described by Amann et al. (1990). The probes used for the hybridization of
230 the bacterial cells are listed in Table S1, more detailed information is available at

231 probeBase (Loy et al., 2007). All probes were commercially synthesized and 5' labeled
232 with either fluorochromes FITC (Fluorescein-5-isocyanate) or Cy3 (Carbocyanine 3).
233 The DNA was detected by using DAPI (4, 6-diamidino-2-phenylindole) as a universal
234 dye. Samples were viewed using an epifluorescence microscope (Axioskop 2 Plus,
235 Zeiss, Germany) coupled with an acquisition system (Coolsnap, Roper Scientific
236 Photometrics).

237

238 **3. RESULTS AND DISCUSSION**

239 **3.1 Origin of the substrate**

240 Mussel cooked wastewater was taken from a 5 L acidogenic reactor in which complex
241 organic compounds (carbohydrates, proteins and lipids) were transformed in order to
242 obtain a VFA-rich stream suitable for PHA production.

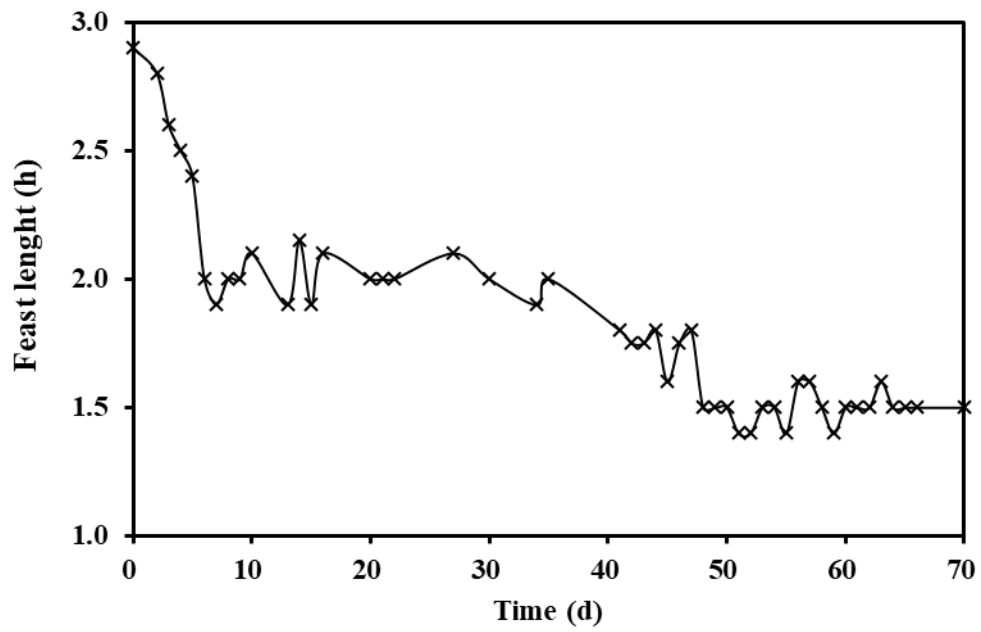
243 **3.2 Improvement of the enrichment due to settling implementation**

244 **3.2.1 Evolution of the enrichment step**

245 The SBR-S was operated for 70 days and the biomass was considered adapted to the
246 new operation after 10 days, when the feast phase length was stabilized as shown in
247 Figure 1.A. The downward evolution of the feast phase length caused a decrease of the
248 feast/cycle length ratio from 0.18 (day 10) to 0.13 (day 65). Considering that values
249 lower than 0.2 - 0.3 were associated to a MMC capable of biopolymer storage (Oliveira
250 et al., 2017), the simple monitoring of the feast/cycle length ratio evidenced the
251 improvement of the selection of accumulating bacteria in the MMC after the
252 implementation of the settling stage.

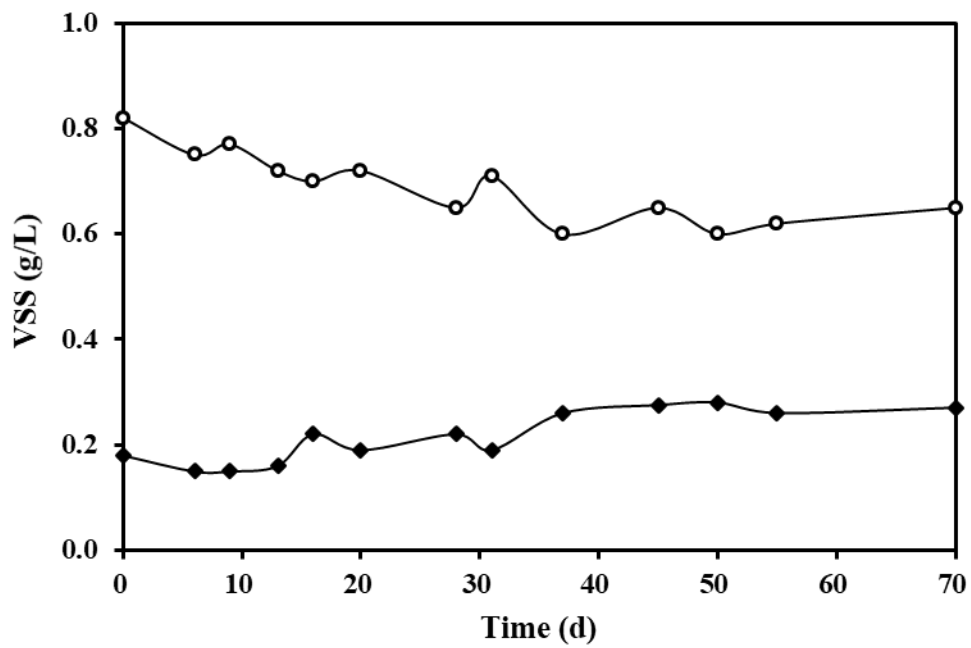
253

A)



254

B)



255

256 **Figure 1.** Evolution in the SBR-S operational period of: A) the feast phase length (x) and B) the
257 VSS concentrations inside the SBR-S at the end of the cycle (the same as in the effluent) at min 705 (○)
258 and in the supernatant discharged after the settling stage (◆) at min 200.

259

260

261 During the first operational days, the VSS concentration inside the SBR-S and end of
262 the cycle (min 705) decreased while its concentration increased in the supernatant
263 discharge (min 200) (Figure 1.B). Then, when the feast length was stabilized, the VSS
264 concentrations were maintained at values of 0.66 ± 0.05 g/L and 0.23 ± 0.04 g/L in the
265 reactor (measurements performed at the end of the cycle) and in the supernatant,
266 respectively. Therefore, not only non-accumulating microorganisms were removed from
267 the system at the end of the cycle at min 705 (wash-out at the end of the famine phase),
268 but also part of them were discharged with the supernatant at min 200 (wash-out at the
269 end of the feast phase).

270 Consequently, apart from the removal of non-desired substances in the supernatant,
271 which favoured the development of non-accumulating microorganisms (proteins and
272 carbohydrates) during the famine phase, the implementation of the settling stage at the
273 end of the feast phase favoured the growth of PHA-accumulating microorganisms in the
274 MMC that could use the accumulated PHA as carbon source for growth (Korkakaki et
275 al., 2016; Kourmentza et al., 2017).

276 The settling stage was implemented after the feast phase, when accumulating bacteria
277 had more intracellular PHA. It is known that the cell weight of these microorganisms is
278 proportional to their cell size and PHA content, which increases the cell density and
279 therefore their settling velocity (Chen et al., 2016). Thus, non-accumulating bacteria
280 presented a lower settleability and they were washed-out with the discharged
281 supernatant after settling. This was in accordance with the results obtained by Chen et
282 al., (2015), who only used acetate as a carbon source (there was no residual COD
283 present in the experiments) in such a way that the improvement of the selection capacity
284 could only be attributed to differences in the cell density that led to physical selection.

285

286 **3.2.2 Enrichment cycle profile and kinetics with (SBR-S) and without (SBR-I)**
287 **settling phase**

288 The differences in the cycle profile between SBR-I and SBR-S can be seen in Figure 2.
289 In the case of SBR-I, the DO concentration after feeding decreased, corresponding to
290 VFA depletion during the feast phase, and then increased during the famine phase due
291 to exhaustion of external carbon source (Figure 2.A).

292 When the settling stage was implemented in the SBR-S, the aeration was stopped to
293 settle the biomass and then, the supernatant was discharged in the absence of oxygen.
294 For this reason, the DO concentration profile showed a strong decrease between the
295 feast and the famine phases (Figure 2.B). Furthermore, it can be observed that the
296 period of VFA consumption was reduced from 3 h in the SBR-I (Figure 2.A) to less
297 than 1 h at day 62 of operation in the SBR-S (Figure 2B), which implied a faster PHA
298 accumulation.

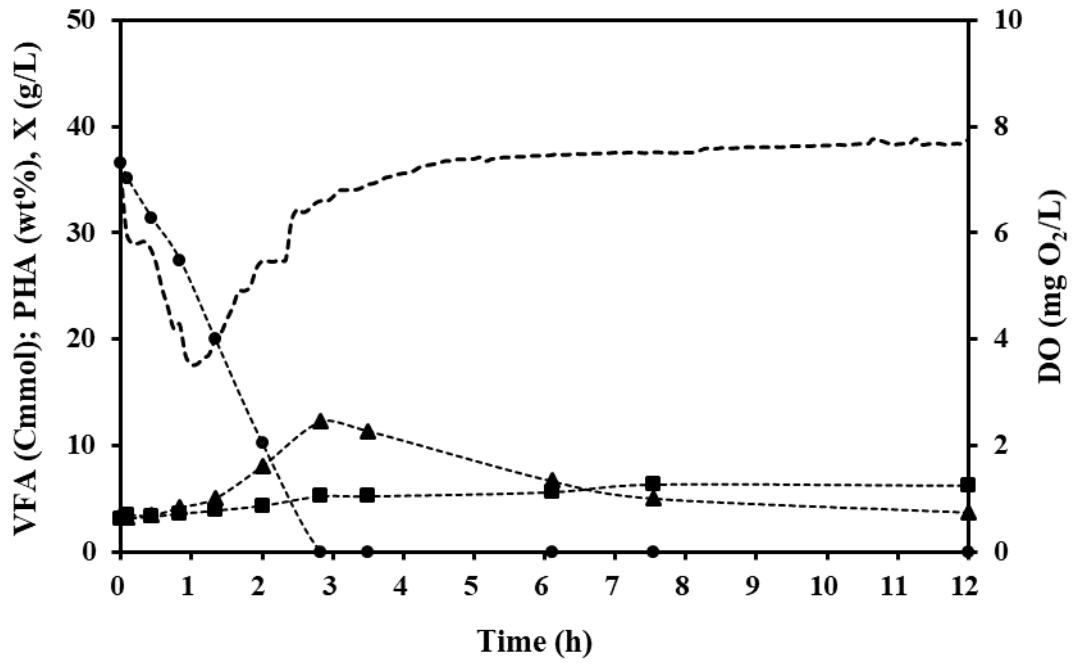
299 To quantify this effect Table 1.A compares the kinetics of SBR-I and SBR-S at day 62.
300 Despite both MMC showed similar specific substrate uptake rates ($q_{VFA} = 0.26-0.27$
301 $Cmmol_{VFA}/(Cmmol_X \cdot h)$), an increase on the q_{PHA} from 0.07 to 0.22
302 $Cmmol_{VFA}/(Cmmol_X \cdot h)$ was observed. Consequently, a higher PHA production yield
303 ($Y_{PHA} = 0.80 Cmmol_{PHA}/h$) and a higher quantity of PHA accumulated (18.32 wt%)
304 were obtained.

305 These results correlate with the downward trend of the feast phase length (Figure 1) and
306 indicate a progressive enhancement on PHA-accumulating microorganisms selection
307 with the implementation of the settling phase.

308

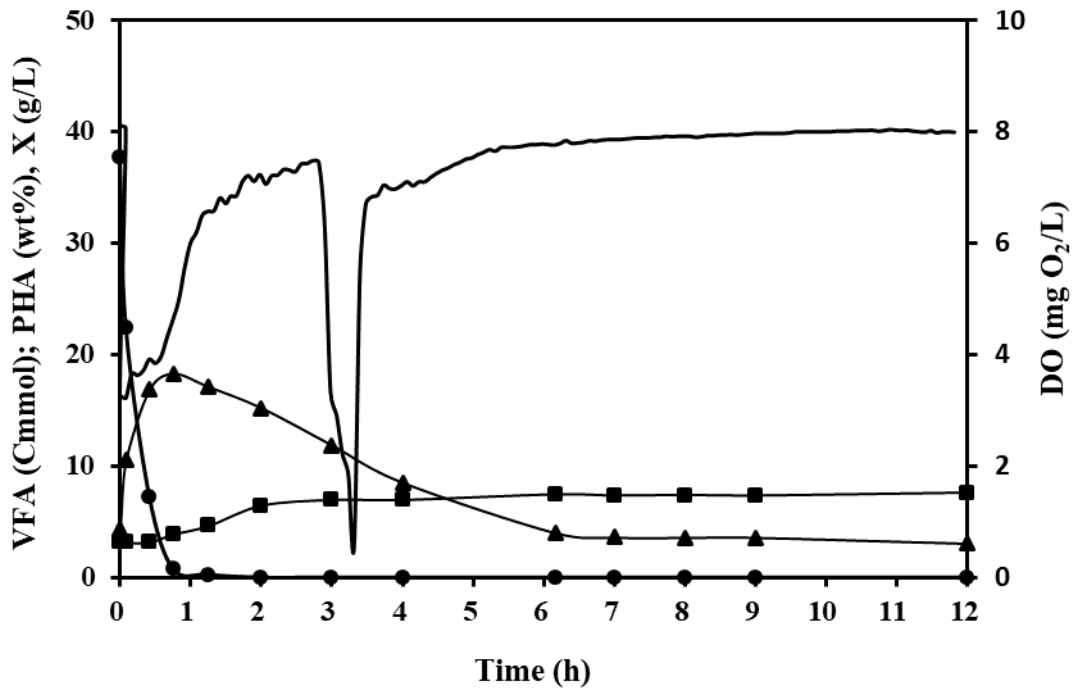
309

A)



310

B)



311

312

313

314

315

316

Figure 2. Evolution of the parameters monitored in representative enrichment cycles: DO (-), VFA (●), X (■) and percentage of PHA accumulated (wt%) (▲). A) Reactor operated without settling stage (SBR-I, - - -) at the moment of inoculum collection. B) Reactor operated with settling stage (SBR-S, —) at day 62 of operation.

317 **Table 1.** Comparison of experimental kinetic parameters and yields of: A) enrichment reactors
 318 operated with (SBR-S) and without settling stage (SBR-I). B) accumulation essays with enriched biomass
 319 from the reactors operated with (FBR-S) and without settling stage (FBR-I).

A)	SBR-I		SBR-S	
			Day 24	Day 62
Feast lenght (h)	2.62 ± 0.10		2.00	1.50
q_{VFA} (Cmmol VFA/Cmmol X·h)	0.26 ± 0.06		0.22	0.27
q_{PHA} (Cmmol PHA/Cmmol X·h)	0.07 ± 0.02		0.14	0.22
q_{HB} (Cmmol HB/Cmmol X·h)	0.06 ± 0.01		0.12	0.15
q_{HV} (Cmmol HV/Cmmol X·h)	0.01 ± 0.01		0.02	0.07
Y_{PHA} (Cmmol PHA/Cmmol VFA)	0.32 ± 0.21		0.61	0.80
max. PHA (wt%)	12.80 ± 0.76		14.77	18.32
HB:HV	88:12 ± 6:6		88:12	70:30

320

B)	FBR-I		FBR-S	
			Day 35	Day 64
q_{VFA} (Cmmol VFA/Cmmol X·h)	0.20		0.30	0.26
q_{PHA} (Cmmol PHA/Cmmol X·h)	0.10		0.14	0.19
q_{HB} (Cmmol HB/Cmmol X·h)	0.08		0.12	0.14
q_{HV} (Cmmol HV/Cmmol X·h)	0.02		0.02	0.05
Y_{PHA} (Cmmol PHA/Cmmol VFA)	0.48		0.49	0.72
max. PHA (wt%)	40.87		44.28	59.92
HB:HV	83:17		82:18	70:30
q_{VFA} (Cmmol VFA/Cmmol X·h)	0.20		0.30	0.26

321 3.2.3 Organic matter balance

322 The pre-acidified cooked mussel processing wastewater used as feedstock contained
 323 two different carbon sources: (1) preferred substrates that are readily available and can
 324 be efficiently converted into PHA by PHA producers (desirable VFA) and (2)
 325 compounds that constitute a carbon source that allows non-accumulating
 326 microorganisms growth (non-desirable carbohydrates and proteins) (Valentino et al.,
 327 2017).

328 The carbon balance of these compounds (detailed in Table S2 of Supplementary
 329 Material) was calculated (as sCOD) during the operational enrichment cycle of the

330 SBR-S: between the beginning of the cycle (Initial), the supernatant discharge after
331 settling (Supernatant) and the end of the cycle (Withdrawal). It was observed an
332 effective removal of non-desired carbon sources with the implementation of the settling
333 stage. In the supernatant were discharged proteins and to a lesser extent carbohydrates
334 (40.16 ± 8.15 % and 34.55 ± 10.13 % of the present at the beginning of the cycle,
335 respectively), which were in a much lower concentration.

336 The concentration of proteins and carbohydrates inside the reactor before settling and
337 after refilling decreased from 120 – 215 mg/L to 60 – 110 mg/L (Figure 3.A) and from
338 20 – 40 mg/L to 15 – 30 mg/L (Figure 3.B) respectively. It should be pointed out that
339 the refilling stream (from the previous cycle effluent) presented low carbohydrates
340 concentrations (14.57 ± 2.58 mg/L) and normally there were no proteins due to their
341 hydrolysis into NH_4^+ , except in isolated cases in which it was measured concentrations
342 of 5 – 10 mg/L. Therefore, the supernatant discharge promoted the removal of
343 substances that could favour the development of non-accumulating microbial
344 populations.

345

346

347

348

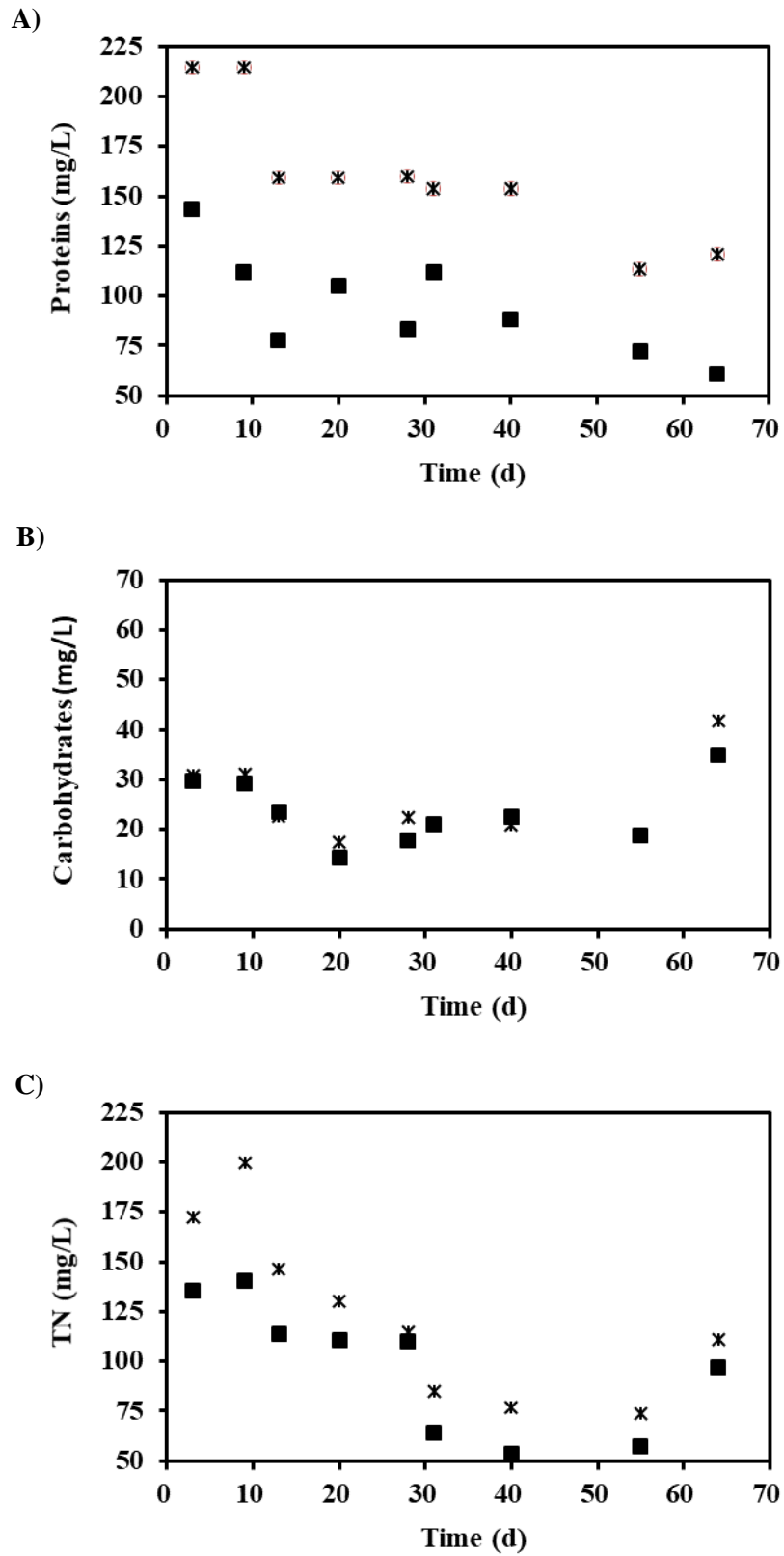


Figure 3. Proteins A), carbohydrates B) and TN C) concentrations before settling (*) and after refilling (■) in the SBR-S reactor.

349 **3.2.4 Nitrogen balance**

350 Nitrogen balances of enrichment were calculated in the SBR-S (more information is
351 detailed in Table S3 and Table S4 of Supplementary Material) showing that 41 – 65 %
352 of the TN present at the beginning of the cycle was discharged with the supernatant
353 after the settling stage. It was also observed that approximately 15 % of the TN present
354 at the beginning of the cycle was consumed during the feast phase, whereas 50 % of the
355 TN present after the reactor refilling was consumed during the famine phase.

356 TN removal with supernatant discharge could limit nutrients availability during the
357 famine phase (when PHA accumulating microorganisms used the accumulated carbon
358 source (PHA) for growth) whereas it was still present during the feast phase (when non-
359 storing microorganisms could use non-desired carbon sources for growth) negatively
360 affecting the enrichment of the system (Figure 3.C). However, refilling provides the
361 SBR with nutrients that lack in the famine phase. In fact, if comparing the reactors with
362 (SBR-S) and without (SBR-I) settling, there was no evidence of a negative effect on the
363 enrichment of the system due to nitrogen removal with supernatant discharge (Table 1).

364 These results controvert the advantages of the carbon-nitrogen uncoupled systems, in
365 which the development of non-accumulating microorganisms was observed to be
366 restricted by applying nitrogen deficiency during the feast phase, resulting in higher
367 PHA production yields and productivities compared to conventional ADF systems
368 (Kourmentza et al., 2017). It is presumed that the decoupling of the system could further
369 improve the enrichment of the MMC. However, the complex and changeable
370 characteristics of the feedstock would surely make it difficult to implement a system
371 like this with such a substrate. It would be necessary to add a pre-treatment of the
372 substrate to remove the ammonium content and later, if possible, recover the previously
373 removed ammonium and reintroduce it in the system, to have nutrient availability

374 during the famine. If not, it would be necessary to add an external nitrogen source
375 which, in addition to the needed pre-treatment, could have an important economic
376 impact in the process.

377 **3.2.5 Considerations for the settling stage implementation**

378 It is necessary to point out that the supernatant should be treated before discharge
379 because of the COD and TN content. It could also be considered its possible reuse or
380 valorization as a fertilizer due to the high NH_4^+ concentration. However, this effluent is
381 also characterized by a high salinity because of the nature of the industrial cooked
382 mussel process, which could be an important hindrance. Regarding economic
383 considerations, settling implementation will presumably lead to an increase in the costs
384 due to the need for an extra pump for recirculation. However, 20 % and 25 % increases
385 of PHA accumulation and PHA production yield, respectively, are expected to
386 compensate investment costs. Operational costs mainly concerning energy requirements
387 for pumping, might be compensated with the lack of aeration during the settling stage.

388 The results obtained suggested an enrichment of the MMC in PHA-accumulating
389 bacteria and therefore an optimization of the system due to the implementation of the
390 settling stage. Moreover, it was observed a reduction of the feast phase length from 3.0
391 to 1.5 hours because of the enrichment of the MMC. Therefore, in order to discharge the
392 supernatant just after VFA depletion and avoid the consumption of the remaining
393 carbon sources (proteins and carbohydrates), which are preferably used for growth of
394 non-accumulating bacteria, the pre-settling reaction stage could be reduced from 165
395 min (imposed in the present SBR-S operation) to 90 minutes. It was also observed an
396 improvement of the enriched biomass settleability and therefore a higher settling
397 velocity of the enriched culture, which suggested a possible reduction of the settling
398 stage length. This coincided with the results obtained by (Korkakaki et al., 2016), who

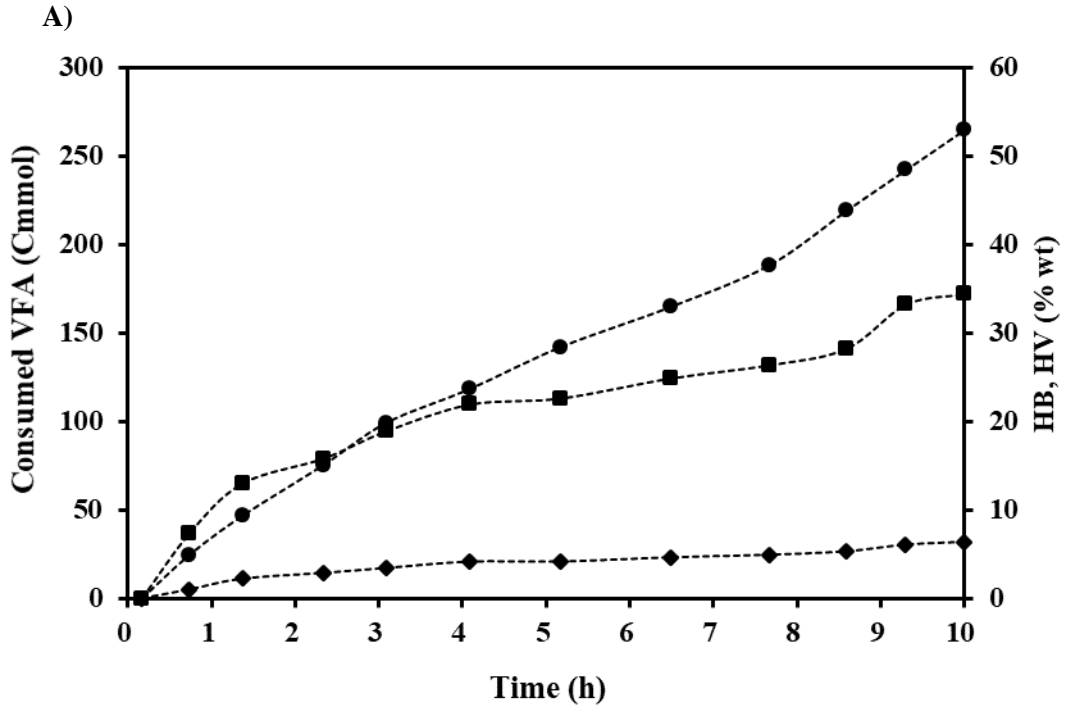
399 observed compaction of the flocs due to their selection after settling implementation and
400 removal of suspended cells.

401 **3.3 Effect of MMC selection on the maximum PHA accumulation capacity**

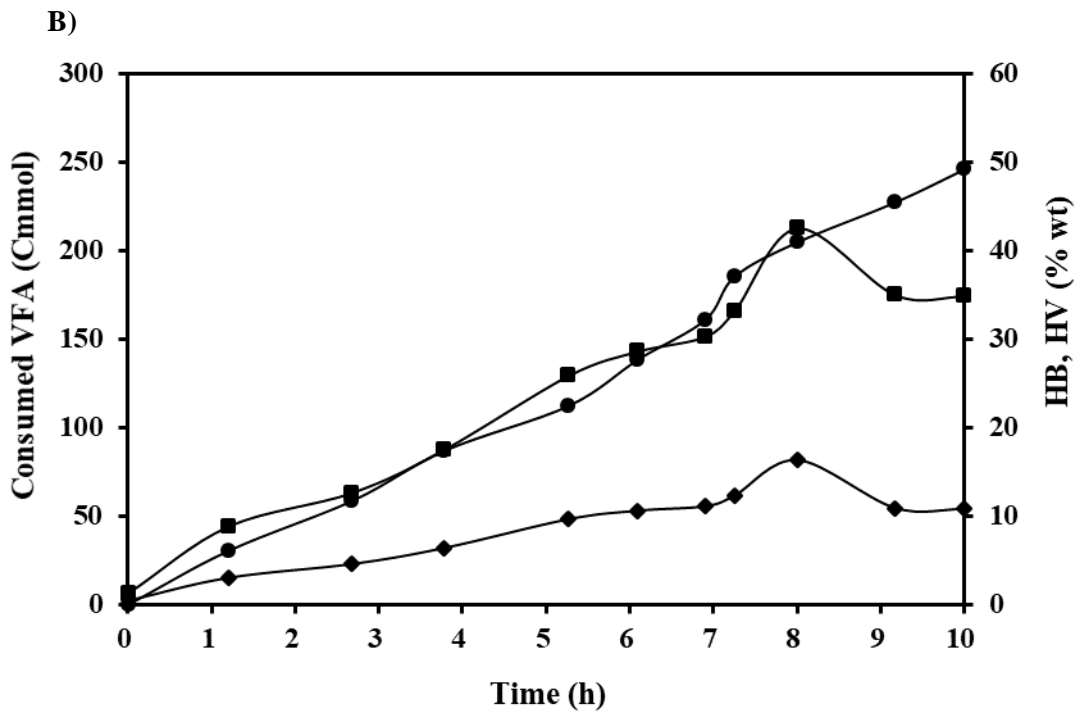
402 To determine the effects of settling in the maximum PHA-accumulation capacity of the
403 MMC, discontinuous accumulation assays were carried out with biomass from SBR-S
404 (FBR-S) and compared with previous assays with biomass from SBR-I (FBR-I).

405 Results of the accumulation assays with biomass from both reactors are considered in
406 Figure 4. Table 1.B shows the experimental kinetic parameters and yields obtained. The
407 maximum PHA-accumulation capacity (max. PHA) of the MMC notably increased in
408 the FBR-S assays (60 %) in comparison with the FBR-I ones (41 %), which correlated
409 with the higher production yield obtained ($Y_{\text{PHA}} = 0.72 \text{ Cmmol}_{\text{PHA}}/\text{h}$). For similar
410 values of the specific substrate uptake rate (q_{VFA}), the improvement of the enrichment in
411 SBR-S promoted an increase of the specific PHA production rate (q_{PHA}) in the
412 accumulation FBR-S experiments, which indicated the improvement of the efficiency of
413 the global PHA production process. In addition, results showed a positive effect on the
414 accumulation kinetic parameters of the FBR-S between days 35 and 64, which
415 correlates with the progressive enhancement of the enrichment SBR-S selection
416 capacity (Table 1.B).

417



418



419

420 **Figure 4.** Evolution of the parameters monitored in accumulation essays (FBR) performed with
 421 enriched biomass: VFA (●) and percentage of accumulated PHB (■) and PHV (◆). A) Reactor operated
 422 without settling stage (FBR-I, - - -) at the moment of inoculum collection. B) Reactor operated with
 423 settling stage (FBR-S, —) at day 64.

424

Table 2. Data from accumulation essays carried out with biomass obtained under different enrichment strategies.

MMC origin & Enrichment strategy	Feedstock	$Y_{PHA/S}$ (Cmmol PHA/ Cmmol S) Max. PHA (wt%) q_{PHA} (CmmolPHA/Cmmol X·h)	Reference
Activated sludge ADF without settling	VFA mixture and lactate	$Y_{PHA/S}$: 0.05 – 0.45	Dionisi et al., 2007
Activated sludge ADF without settling	Sodium acetate	Max. PHA: 69.00 – 89.00	Johnson et al., 2009
Water from a river estuary ADF + settling before withdrawal	Sodium acetate, glucose or starch	$Y_{PHA/S}$: 0.60 sodium acetate / 0.54 glucose / 0.30 starch Max. PHA: 64.70 sodium acetate / 60.50 glucose / 23.70 starch	Cui et al., 2016
Activated sludge ADF without and with settling after feast phase	Mixture of sodium acetate and methanol	Max. PHA: 48.00 without settling / 58.00-70.00 with settling	Korkakaki et al., 2016
Activated sludge ADF + settling after feast phase	Nutrients rich fermented centrate sludge	$Y_{PHA/S}$: 0.25 - 0.27 Max. PHA: 17.00 - 39.00	Morgan-Sagastume et al., 2015
Activated sludge ADF uncoupled C and N feeding strategy + settling after feast phase	Industrial soft drink wastewater	Max. PHA: 13.80	Ahmadi et al., 2018
Activated sludge ADF coupled and uncoupled carbon and nitrogen feeding strategy + settling before withdrawal	Fermented cheese whey	$Y_{PHA/S}$: 0.86 coupled / 0.96 uncoupled q_{PHA} : 0.29 coupled / 0.40 uncoupled	Oliveira et al., 2017
Activated sludge ADD (aerobic dinamic discharge) + two settling stages (after feast phase and before withdrawal)	Mixture of sodium acetate, NH_4Cl and KH_2PO_4	q_{PHA} : 0.47 - 1.89	Chen et al., 2016
Enriched biomass from the C-SBR, which was inoculated with activated sludge ADF + settling stage after feast phase	Synthetic VFA mixture mimicking the composition of pre-acidified cooked mussel wastewater	$Y_{PHA/S}$: 0.72 Max. PHA: 59.92 q_{PHA} : 0.19	This work

426 Results obtained in FBR-S are compared in Table 2 with others found in the literature
427 using MMC, real and synthetic feedstocks and different enrichment strategies (coupled
428 and uncoupled systems with and without settling). The results obtained in the present
429 research work are comparable to those reached in the literature using synthetic
430 feedstocks (both for the enrichment of the culture and evaluation of the maximum
431 accumulation capacity) (Cui et al., 2016; Johnson et al., 2009; Korkakaki et al., 2016;
432 Dionisy et al., 2007), and higher to the obtained in systems fed with real substrates
433 (Ahmadi et al., 2018; Morgan-Sagastume et al., 2015) in spite of the complexity and
434 high salinity of the pre-acidified cooked mussel wastewater. It has been reported that
435 NaCl concentrations cause a severe effect over the respiration activity, which
436 diminishes with the increase of salt ($IC_{50} = 5 \text{ g NaCl/L}$ in a MMC non-adapted to
437 salinity) and negatively affects the PHA accumulation (Palmeiro-Sánchez et al., 2016a).
438 Biopolymers obtained in FBR-S assays were composed by HB and HV monomers with
439 a HB:HV ratio of 70:30 whereas in the FBR-I assays HV monomer was in a lower
440 proportion (HB:HV ratio of 87:13). It has been previously reported that the PHA
441 composition is a function of the VFA profile in the feed, where the HV fraction
442 increases with the abundance of VFAs with an odd number of carbon atoms such as
443 propionate and valerate (Albuquerque et al., 2013, 2007). However, in the present study
444 both reactors were fed with the same substrate, which was mainly composed by acetic
445 acid ($63.85 \pm 5.16 \%$), but also propionic ($21.76 \pm 7.82 \%$), butyric ($13.49 \pm 2.59 \%$)
446 and valeric acids ($0.89 \pm 1.53 \%$). Small variations observed in the VFA profile during
447 the operation were a consequence of the changeable characteristics of the influent.
448 Therefore, changes could be a consequence of possible variations in the microbial
449 community due to settling implementation since there is a correlation between the
450 microbial community structure and the biopolymer composition (Carvalho et al., 2014).

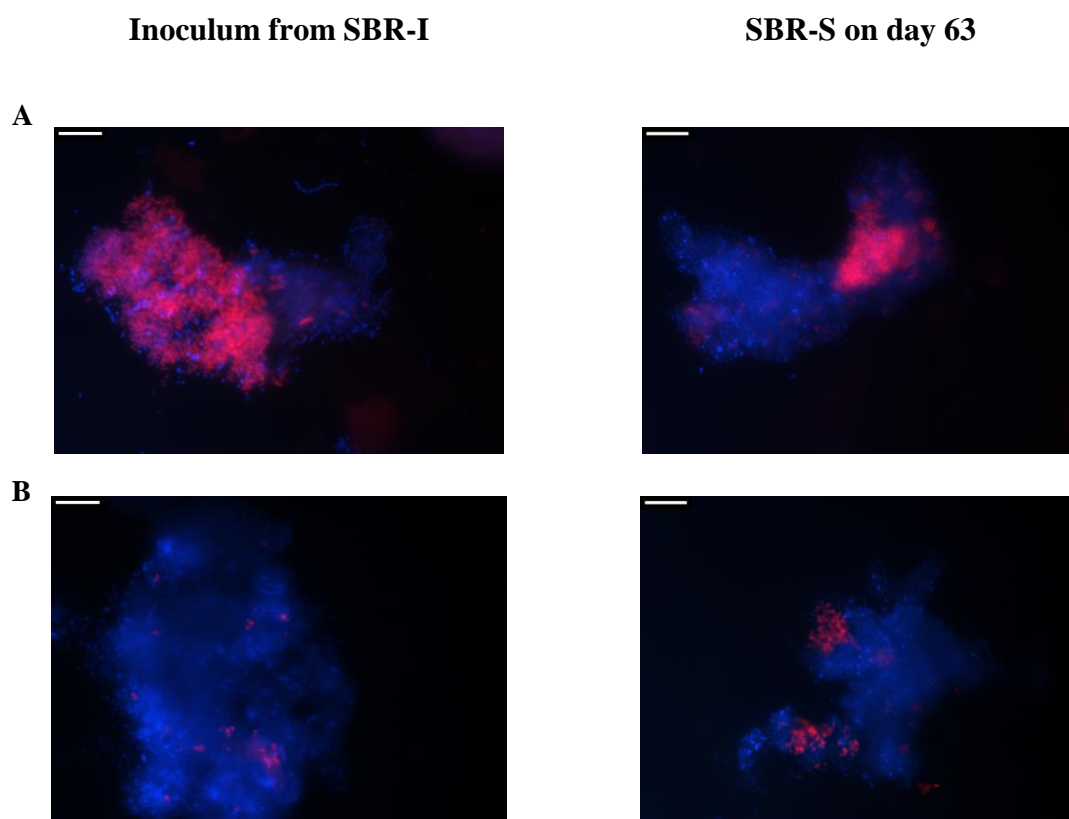
451 **3.4 Variations in the MMC enhanced the obtention of different biopolymers from**
452 **the same influent**

453 The MMC was characterized by the presence of heterotrophic bacteria with high PHA
454 accumulation capacity. Results obtained by FISH technique showed that
455 microorganisms present in the inoculum of the SBR-S mainly belonged to phyla
456 *Bacteroidetes* and *Proteobacteria*, and this latter included microorganisms from genera
457 *Comamonas*, *Azoarcus* and *Thauera*. All these identified microorganisms have been
458 previously reported as PHA-storing bacteria in MMC (Morgan-Sagastume et al., 2015)

459 Changes in the microbial community were observed at day 63 of SBR-S (Figure 5).
460 Genus *Paracoccus* sharply increased whereas the abundance of genera *Comamonas*
461 decreased. Those populations that reduced their abundances, even though they were
462 reported as PHA-storing microorganisms, probably accumulated PHA in less
463 proportion. Therefore, they had slower settling velocity and were washed-out with the
464 supernatant discharged after the settling stage. These changes in the MMC composition
465 presumably modified the substrate uptake preferences, which could explain the
466 variations observed in the HB:HV ratio. Thus, as previously reported, the same
467 substrate could result in PHA with different %HV depending on the microbial
468 populations and their metabolic characteristics (Carvalho et al., 2014). This succession
469 of dominant microbe from *Paracoccus* to *Comamonas* could not be attributed to the
470 high salinity in the wastewater. Thus, NaCl concentrations in the influent of the SBR-I
471 (5 – 13 g NaCl/L), from which was taken the inoculum, were similar to those of the
472 SBR-S (4 – 12 g NaCl/L).

473 Albuquerque et al., (2013) mimicked the simultaneous presence of different substrates
474 in a bioreactor and observed clear substrate-uptake preferences in a PHA-storing

475 community. All the populations could take up several substrates simultaneously but
476 there was a substrate preference: acetate was mainly taken up by *Azoarcus* and
477 *Paracoccus*; propionate by *Paracoccus*; butyrate by *Thauera*; and *Paracoccus* and
478 valerate by *Paracoccus* (Albuquerque et al., 2013; Morgan-Sagastume et al., 2016). The
479 generally accepted metabolic pathway for PHA synthesis from organic acids assumes
480 acetate and butyrate as HB precursors and propionate and valerate as HV precursors
481 (Duque et al., 2014). According to this, VFA composition in the influent (63.85 ± 5.16
482 % acetic acid, 21.76 ± 7.82 % propionic acid, 13.49 ± 2.59 % butyric acid and $0.89 \pm$
483 1.53 % valeric acid) explains the high HB proportion in the HB:HV ratio (70:30).



484

485 **Figure 5.** FISH images of the enriched biomass from the SBR-I (inoculum of SBR-S) and SBR-S at
486 day 63. A) *Comamonas* (Cte: Cy3, red) and all DNA (DAPI, blue) and B) *Paracoccus* (Par1244; Cy3,
487 red) and all DNA (DAPI, blue). The bar represents 10 μm.

488

489 The pronounced increase observed in the presence of genus *Paracoccus* in the SBR-S
490 could derive on a higher propionate and valerate affinity of the whole microbial
491 community in comparison with the inoculum (from SBR-I). Consequently, this result
492 explains the bigger HV proportion in the HB:HV ratio of SBR-S (70:30) compared with
493 the SBR-I (87:13) (Table 1.A). In addition, *Thauera* abundance was found to play an
494 important role in the HV content of the biopolymer, even more than the propionate +
495 valerate fraction. This might indicate that distinct metabolic pathways are prevalent in
496 each microbial group for PHA production (Carvalho et al., 2014). However, a high HB
497 proportion was still maintained, which correlates with the observed by Albuquerque et
498 al., (2013) and Carvalho et al., (2014). These authors stated that *Paracoccus*
499 enrichments favour the storage of VFA as PHA polymers with a higher HB content.

500 PHA properties are generally tailored using specific substrates to obtain copolymers
501 with different monomer compositions (Duque et al., 2014; Palmeiro-Sánchez et al.,
502 2016b). In addition, it was also studied the possibility of manipulating the biopolymer
503 composition without changes in the feedstock. Albuquerque et al., (2011) demonstrated
504 that the feeding regime (pulsed versus continuous) of the accumulation reactor affected
505 polymer composition and observed that continuous feeding resulted in a higher HV
506 content using the same feedstock. In the present research work, the implementation of a
507 settling stage generated shifts in the microbial community, which directly correlated
508 with the type and characteristics of the PHA produced, due to the link existent between
509 the microorganisms present in the mixed culture and their carbon substrate-uptake
510 preferences. Therefore, the results of the present study showed the possibility of
511 modifying the biopolymer properties through the imposition of changes in the SBR
512 operational cycle without changing the substrate composition or the feeding strategy in
513 the accumulation reactor. In this particular case, settling implementation caused an

514 increase in the HV fraction. This derived on a reduction of the biopolymer crystallinity
515 and the melting and glass transition temperatures, which ultimately enhances the
516 biopolymer flexibility and processability (Dias et al., 2006).

517

518 **4. CONCLUSIONS**

519 The addition of a settling phase to the operational cycle (at the end of the feast phase) in
520 an enrichment SBR for PHA production, fed with pre-acidified complex saline
521 wastewater generated in mussel cookers, was evaluated. The enrichment of the MMC
522 was improved by the wash-out of microbial populations with lower or no PHA-storage
523 capacity after the feast phase. Moreover, the discharge of the supernatant after the feast
524 phase favoured the removal of substances that enhanced the development of non-
525 accumulating microorganisms. Variations in the microbial community were observed
526 and genus *Paracoccus* notably increased in abundance, whereas genera *Comamonas*
527 decreased. The implementation of the settling stage improved the maximum PHA
528 storage capacity (from 40 up to 60 wt%) and varied the co-polymer composition in
529 terms of HB:HV ratio (HV proportion increased from 17 to 30 %).

530

531 **5. ACKNOWLEDGEMENTS**

532 This research was supported by the Spanish Government (AEI) through the
533 TREASURE project [CTQ2017-83225-C2-1-R]. Lucía Argiz is a Xunta de Galicia
534 fellow (2019), this grant is cofunded by the operative program FSE Galicia 2014-2020.
535 Moreover, authors would like to thank the EU and the AEI for funding, in the frame of
536 the collaborative international Consortium AquaVal project, [PCIN-2017-047], financed
537 under the ERA-NET WaterWorks2015 Cofunded Call. This ERA-NET is an integral

538 part of the 2016 Joint Activities developed by the Water Challenges for a Changing
539 World Joint Programme Initiative (Water JPI). The authors belong to CRETUS
540 Strategic Partnership (ED4331e 2018/01) and the Galician Competitive Research Group
541 GRC ED431C 2017/29. All these programs are co-funded by the FEDER (EU).

542

543 **6. REFERENCES**

544 Ahmadi, F., Zinatizadeh, A.A., Asadi, A., 2018. PHA production from wastewater by
545 mixed microbial culture under short- term microbial enrichment 9, 389–391.
546 <https://doi.org/10.22126/arww.2018.863>

547 Albuquerque, M.G.E., Carvalho, G., Kragelund, C., Silva, A.F., Barreto Crespo, M.T.,
548 Reis, M.A.M., Nielsen, P.H., 2013. Link between microbial composition and
549 carbon substrate-uptake preferences in a PHA-storing community. *ISME J.* 7, 1–
550 12. <https://doi.org/10.1038/ismej.2012.74>

551 Albuquerque, M.G.E., Concas, S., Bengtsson, S., Reis, M.A.M., 2010. Mixed culture
552 polyhydroxyalkanoates production from sugar molasses: The use of a 2-stage
553 CSTR system for culture selection. *Bioresour. Technol.* 101, 7112–7122.
554 <https://doi.org/10.1016/j.biortech.2010.04.019>

555 Albuquerque, M.G.E., Eiroa, M., Torres, C., Nunes, B.R., Reis, M.A.M., 2007.
556 Strategies for the development of a side stream process for polyhydroxyalkanoate
557 (PHA) production from sugar cane molasses. *J. Biotechnol.* 130, 411–421.
558 <https://doi.org/10.1016/j.jbiotec.2007.05.011>

559 Albuquerque, M.G.E., Martino, V., Pollet, E., Avérous, L., Reis, M.A.M., 2011. Mixed
560 culture polyhydroxyalkanoate (PHA) production from volatile fatty acid (VFA)-
561 rich streams: Effect of substrate composition and feeding regime on PHA
562 productivity, composition and properties. *J. Biotechnol.* 151, 66–76.
563 <https://doi.org/10.1016/j.jbiotec.2010.10.070>

564 Amann, R.L., Krumholz, L., Stahl, D.A., 1990. Fluorescent-oligonucleotide probing of
565 whole cells for determinative, phylogenetic, and environmental studies in
566 microbiology. *J. Bacteriol.* 172, 762–770. [https://doi.org/10.1128/jb.172.2.762-](https://doi.org/10.1128/jb.172.2.762-770.1990)
567 [770.1990](https://doi.org/10.1128/jb.172.2.762-770.1990)

- 568 Bower, C.E., Holm-Hansen, T., 1980. A Salicylate–Hypochlorite Method for
569 Determining Ammonia in Seawater. *Can. J. Fish. Aquat. Sci.* 37, 794–798.
570 <https://doi.org/10.1139/f80-106>
- 571 Carvalho, G., Oehmen, A., Albuquerque, M.G.E., Reis, M.A.M., 2014. The relationship
572 between mixed microbial culture composition and PHA production performance
573 from fermented molasses. *N. Biotechnol.* 31, 257–263.
574 <https://doi.org/10.1016/j.nbt.2013.08.010>
- 575 Chen, Z., Guo, Z., Wen, Q., Huang, L., Bakke, R., Du, M., 2016. Modeling
576 polyhydroxyalkanoate (PHA) production in a newly developed aerobic dynamic
577 discharge (ADD) culture enrichment process. *Chem. Eng. J.* 298, 36–43.
578 <https://doi.org/10.1016/j.cej.2016.03.133>
- 579 Chen, Z., Guo, Z., Wen, Q., Huang, L., Bakke, R., Du, M., 2015. A new method for
580 polyhydroxyalkanoate (PHA) accumulating bacteria selection under physical
581 selective pressure. *Int. J. Biol. Macromol.* 72, 1329–1334.
582 <https://doi.org/10.1016/j.ijbiomac.2014.10.027>
- 583 Cui, Y.W., Zhang, H.Y., Lu, P.F., Peng, Y.Z., 2016. Effects of carbon sources on the
584 enrichment of halophilic polyhydroxyalkanoate-storing mixed microbial culture in
585 an aerobic dynamic feeding process. *Sci. Rep.* 6. <https://doi.org/10.1038/srep30766>
- 586 Dias, J.M.L., Lemos, P.C., Serafim, L.S., Oliveira, C., Eiroa, M., Albuquerque, M.G.E.,
587 Ramos, A.M., Oliveira, R., Reis, M.A.M., 2006. Recent advances in
588 polyhydroxyalkanoate production by mixed aerobic cultures: From the substrate to
589 the final product. *Macromol. Biosci.* 6, 885–906.
590 <https://doi.org/10.1002/mabi.200600112>
- 591 Duque, A.F., Oliveira, C.S.S., Carmo, I.T.D., Gouveia, A.R., Pardelha, F., Ramos,
592 A.M., Reis, M.A.M., 2014. Response of a three-stage process for PHA production
593 by mixed microbial cultures to feedstock shift: Impact on polymer composition. *N.*
594 *Biotechnol.* 31, 276–288. <https://doi.org/10.1016/j.nbt.2013.10.010>
- 595 Jiang, G., Hill, D.J., Kowalczyk, M., Johnston, B., Adamus, G., Irorere, V., Radecka, I.,
596 2016. Carbon sources for polyhydroxyalkanoates and an integrated biorefinery. *Int.*
597 *J. Mol. Sci.* 17. <https://doi.org/10.3390/ijms17071157>
- 598 Johnson, K., Jiang, Y., Kleerebezem, R., Muyzer, G., Van Loosdrecht, M.C.M., 2009.

599 Enrichment of a mixed bacterial culture with a high polyhydroxyalkanoate storage
600 capacity. *Biomacromolecules* 10, 670–676. <https://doi.org/10.1021/bm8013796>

601 Keshavarz, T., Roy, I., 2010. Polyhydroxyalkanoates: bioplastics with a green agenda.
602 *Curr. Opin. Microbiol.* 13, 321–326. <https://doi.org/10.1016/j.mib.2010.02.006>

603 Korkakaki, E., van Loosdrecht, M.C.M., Kleerebezem, R., 2016. Survival of the fastest:
604 Selective removal of the side population for enhanced PHA production in a mixed
605 substrate enrichment. *Bioresour. Technol.* 216, 1022–1029.
606 <https://doi.org/10.1016/j.biortech.2016.05.125>

607 Kourmentza, C., Plácido, J., Venetsaneas, N., Burniol-Figols, A., Varrone, C., Gavala,
608 H.N., Reis, M.A.M., 2017. Recent Advances and Challenges towards Sustainable
609 Polyhydroxyalkanoate (PHA) Production. *Bioengineering* 4, 55.
610 <https://doi.org/10.3390/bioengineering4020055>

611 Loewus, F.A., 1952. Improvement in Anthrone Method for Determination of
612 Carbohydrates Errors in Volumetric Analysis Arising from Adsorption. *Anal.*
613 *Chem.* 24, 219–219. <https://doi.org/10.1021/ac60061a050>

614 Lowry, O. H.; Rosebrough, N. J.; Farr, A. L.; Randall, R.J., 1951. Protein measurement
615 with the folin phenol reagent. *Anal. Biochem.* 217, 220–230.
616 [https://doi.org/10.1016/0304-3894\(92\)87011-4](https://doi.org/10.1016/0304-3894(92)87011-4)

617 Loy, A., Maixner, F., Wagner, M., Horn, M., 2007. probeBase - An online resource for
618 rRNA-targeted oligonucleotide probes: New features 2007. *Nucleic Acids Res.* 35,
619 800–804. <https://doi.org/10.1093/nar/gkl856>

620 Marang, L., Jiang, Y., Loosdrecht, M.C.M. Van, Kleerebezem, R., 2014. Impact of non-
621 storing biomass on PHA production: An enrichment culture on acetate and
622 methanol. *Int. J. Biol. Macromol.* <https://doi.org/10.1016/j.ijbiomac.2014.04.051>

623 Morgan-Sagastume, F., Hjort, M., Cirne, D., Gérardin, F., Lacroix, S., Gaval, G.,
624 Karabegovic, L., Alexandersson, T., Johansson, P., Karlsson, A., Bengtsson, S.,
625 Arcos-Hernández, M. V., Magnusson, P., Werker, A., 2015. Integrated production
626 of polyhydroxyalkanoates (PHAs) with municipal wastewater and sludge treatment
627 at pilot scale. *Bioresour. Technol.* 181, 78–89.
628 <https://doi.org/10.1016/j.biortech.2015.01.046>

629 Nikodinovic-Runic, J., Guzik, M., Kenny, S.T., Babu, R., Werker, A., O'Connor, K.E.,

630 2013. Carbon-rich wastes as feedstocks for biodegradable polymer
631 (polyhydroxyalkanoate) production using bacteria, 1st ed, *Advances in Applied*
632 *Microbiology*. Elsevier Inc. <https://doi.org/10.1016/B978-0-12-407673-0.00004-7>

633 Oliveira, C.S.S., Silva, C.E., Carvalho, G., Reis, M.A., 2017. Strategies for efficiently
634 selecting PHA producing mixed microbial cultures using complex feedstocks:
635 Feast and famine regime and uncoupled carbon and nitrogen availabilities. *N.*
636 *Biotechnol.* 37, 69–79. <https://doi.org/10.1016/j.nbt.2016.10.008>

637 Palmeiro-Sánchez, T., Fra-Vázquez, A., Rey-Martínez, N., Campos, J.L., Mosquera-
638 Corral, A., 2016a. Transient concentrations of NaCl affect the PHA accumulation
639 in mixed microbial culture. *J. Hazard. Mater.* 306, 332–339.
640 <https://doi.org/10.1016/j.jhazmat.2015.12.032>

641 Palmeiro-Sánchez, T., Oliveira, C.S.S., Gouveia, A.R., Noronha, J.P., Ramos, A.M.,
642 Mosquera-Corral, A., Reis, M.A.M., 2016b. NaCl presence and purification affect
643 the properties of mixed culture PHAs. *Eur. Polym. J.* 85, 256–265.
644 <https://doi.org/10.1016/j.eurpolymj.2016.10.035>

645 Reddy, C.S.K., Ghai, R., Rashmi, Kalia, V.C., 2003. Polyhydroxyalkanoates: An
646 overview. *Bioresour. Technol.* 87, 137–146. [https://doi.org/10.1016/S0960-](https://doi.org/10.1016/S0960-8524(02)00212-2)
647 [8524\(02\)00212-2](https://doi.org/10.1016/S0960-8524(02)00212-2)

648 Samorì, C., Abbondanzi, F., Galletti, P., Giorgini, L., Mazzocchetti, L., Torri, C.,
649 Tagliavini, E., 2015. Bioresource Technology Extraction of polyhydroxyalkanoates
650 from mixed microbial cultures : Impact on polymer quality and recovery 189, 195–
651 202. <https://doi.org/10.1016/j.biortech.2015.03.062>

652 Serafim, L.S., Lemos, P.C., Oliveira, R., Reis, M.A.M., 2004. Optimization of
653 polyhydroxybutyrate production by mixed cultures submitted to aerobic dynamic
654 feeding conditions. *Biotechnol. Bioeng.* 87, 145–160.
655 <https://doi.org/10.1002/bit.20085>

656 Smolders, G.J.F., van der Meij, J., van Loosdrecht, M.C.M., Heijnen, J.J., 1994.
657 Stoichiometric model of the aerobic metabolism of the biological phosphorus
658 removal process. *Biotechnol. Bioeng.* 44, 837–848.
659 <https://doi.org/10.1002/bit.260440709>

660 Valentino, F., Morgan-Sagastume, F., Campanari, S., Villano, M., Werker, A., Majone,

661 M., 2017. Carbon recovery from wastewater through bioconversion into
662 biodegradable polymers. N. Biotechnol. 37, 9–23.
663 <https://doi.org/10.1016/j.nbt.2016.05.007>

664 Zhu, C., Chiu, S., Nakas, J.P., Nomura, C.T., 2013. Bioplastics from waste glycerol
665 derived from biodiesel industry. J. Appl. Polym. Sci. 130, 1–13.
666 <https://doi.org/10.1002/app.39157>

667

1 **Table 1.** Comparison of experimental kinetic parameters and yields of: A) enrichment reactors
 2 operated with (SBR-S) and without settling stage (SBR-I). B) accumulation essays with enriched biomass
 3 from the reactors operated with (FBR-S) and without settling stage (FBR-I).

A)	SBR-I	SBR-S	
		Day 24	Day 62
Feast lenght (h)	2.62 ± 0.10	2.00	1.50
q _{VFA} (Cmmol VFA/Cmmol X·h)	0.26 ± 0.06	0.22	0.27
q _{PHA} (Cmmol PHA/Cmmol X·h)	0.07 ± 0.02	0.14	0.22
q _{HB} (Cmmol HB/Cmmol X·h)	0.06 ± 0.01	0.12	0.15
q _{HV} (Cmmol HV/Cmmol X·h)	0.01 ± 0.01	0.02	0.07
Y _{PHA} (Cmmol PHA/Cmmol VFA)	0.32 ± 0.21	0.61	0.80
max. PHA (wt%)	12.80 ± 0.76	14.77	18.32
HB:HV	88:12 ± 6:6	88:12	70:30

4

B)	FBR-I	FBR-S	
		Day 35	Day 64
q _{VFA} (Cmmol VFA/Cmmol X·h)	0.20	0.30	0.26
q _{PHA} (Cmmol PHA/Cmmol X·h)	0.10	0.14	0.19
q _{HB} (Cmmol HB/Cmmol X·h)	0.08	0.12	0.14
q _{HV} (Cmmol HV/Cmmol X·h)	0.02	0.02	0.05
Y _{PHA} (Cmmol PHA/Cmmol VFA)	0.48	0.49	0.72
max. PHA (wt%)	40.87	44.28	59.92
HB:HV	83:17	82:18	70:30
q _{VFA} (Cmmol VFA/Cmmol X·h)	0.20	0.30	0.26

5

6

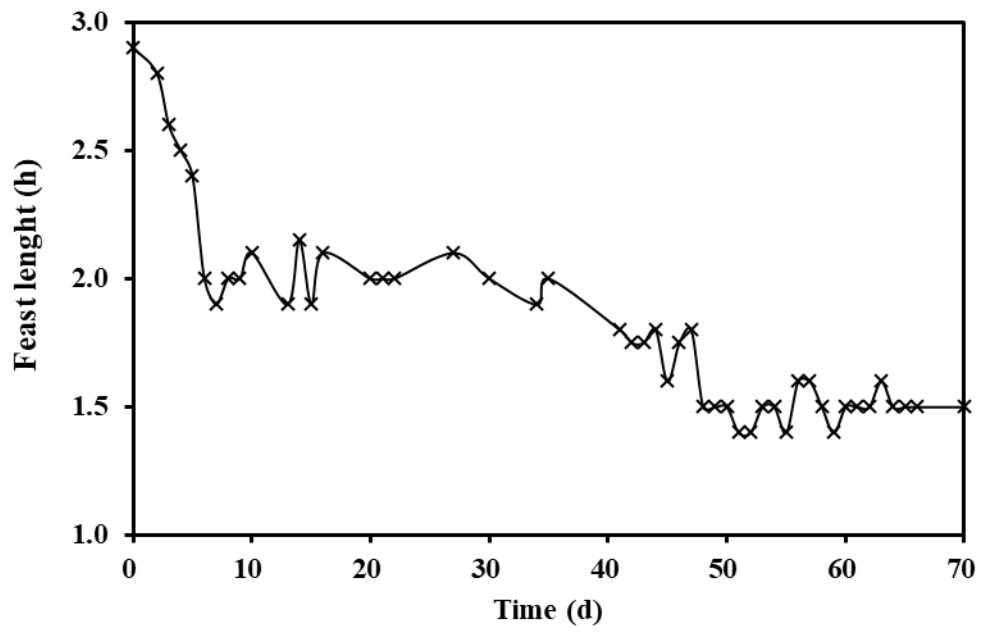
7

Table 2. Data from accumulation essays carried out with biomass obtained under different enrichment strategies.

MMC origin & Enrichment strategy	Feedstock	$Y_{PHA/S}$ (Cmmol PHA/ Cmmol S) Max. PHA (wt%) q_{PHA} (CmmolPHA/Cmmol X·h)	Reference
Activated sludge ADF without settling	VFA mixture and lactate	$Y_{PHA/S}$: 0.05 – 0.45	Dionisi et al., 2007
Activated sludge ADF without settling	Sodium acetate	Max. PHA: 69.00 – 89.00	Johnson et al., 2009
Water from a river estuary ADF + settling before withdrawal	Sodium acetate, glucose or starch	$Y_{PHA/S}$: 0.60 sodium acetate / 0.54 glucose / 0.30 starch Max. PHA: 64.70 sodium acetate / 60.50 glucose / 23.70 starch	Cui et al., 2016
Activated sludge ADF without and with settling after feast phase	Mixture of sodium acetate and methanol	Max. PHA: 48.00 without settling / 58.00-70.00 with settling	Korkakaki et al., 2016
Activated sludge ADF + settling after feast phase	Nutrients rich fermented centrate sludge	$Y_{PHA/S}$: 0.25 - 0.27 Max. PHA: 17.00 - 39.00	Morgan-Sagastume et al., 2015
Activated sludge ADF uncoupled C and N feeding strategy + settling after feast phase	Industrial soft drink wastewater	Max. PHA: 13.80	Ahmadi et al., 2018
Activated sludge ADF coupled and uncoupled carbon and nitrogen feeding strategy + settling before withdrawal	Fermented cheese whey	$Y_{PHA/S}$: 0.86 coupled / 0.96 uncoupled q_{PHA} : 0.29 coupled / 0.40 uncoupled	Oliveira et al., 2017
Activated sludge ADD (aerobic dinamic discharge) + two settling stages (after feast phase and before withdrawal)	Mixture of sodium acetate, NH_4Cl and KH_2PO_4	q_{PHA} : 0.47 - 1.89	Chen et al., 2016
Enriched biomass from the C-SBR, which was inoculated with activated sludge ADF + settling stage after feast phase	Synthetic VFA mixture mimicking the composition of pre-acidified cooked mussel wastewater	$Y_{PHA/S}$: 0.72 Max. PHA: 59.92 q_{PHA} : 0.19	This work

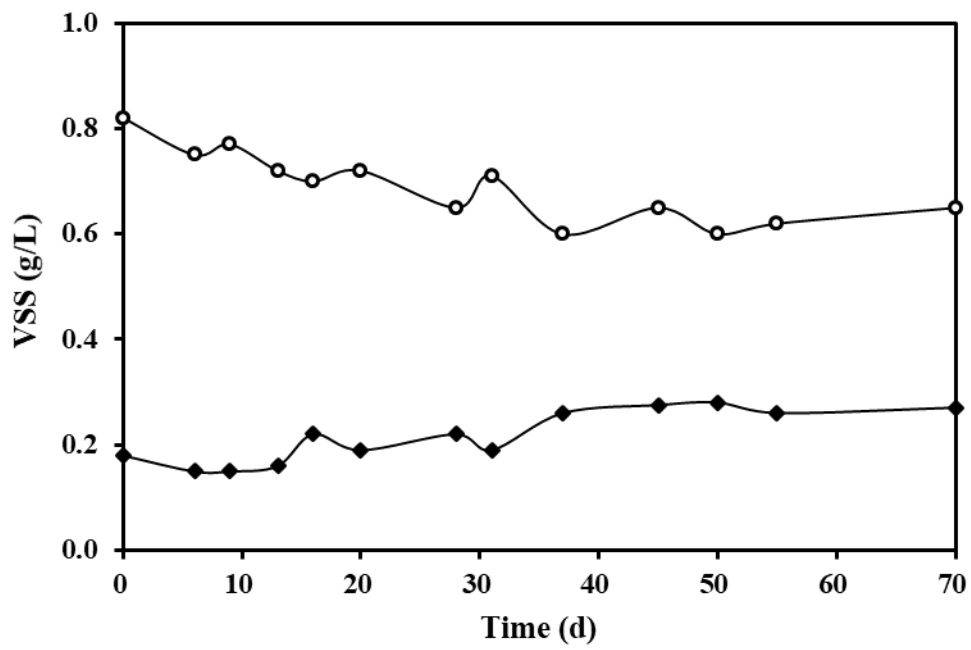
1 **Figure 1**

2 A)



3

B)



4

5

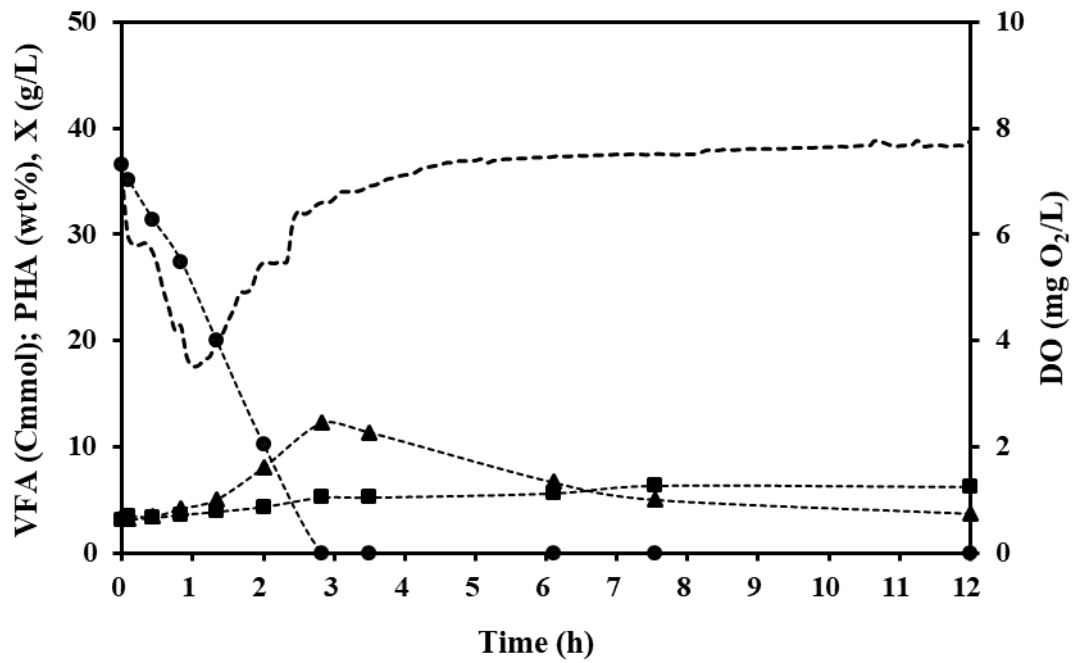
6

7

8

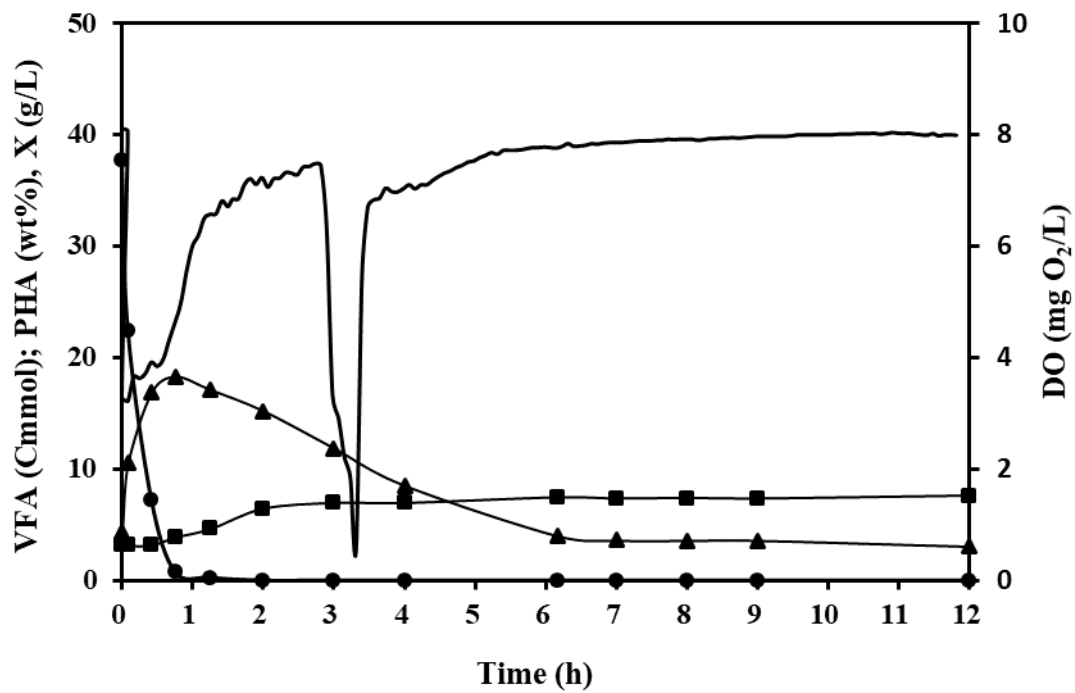
9 **Figure 2**

A)



10

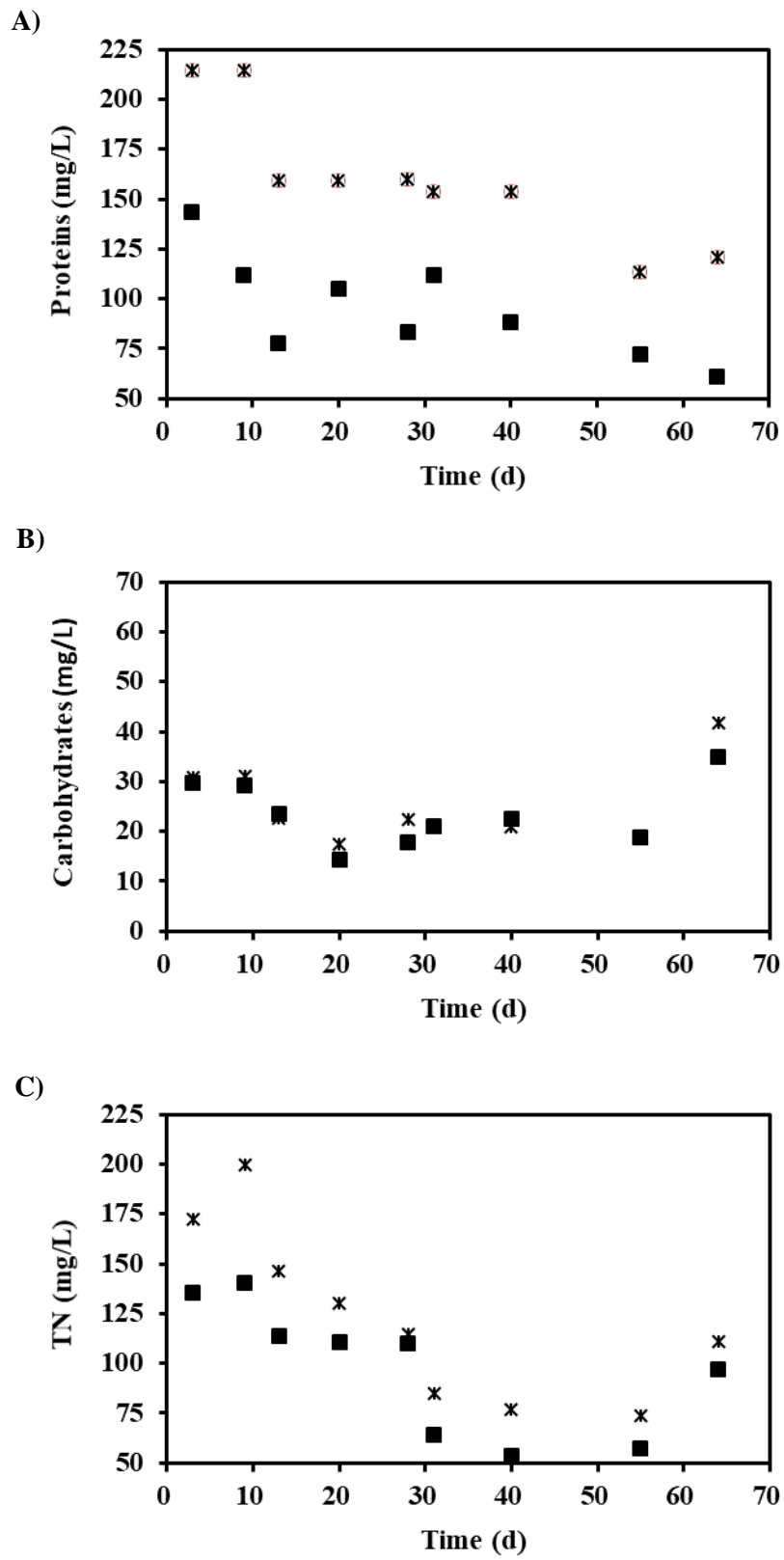
B)



11

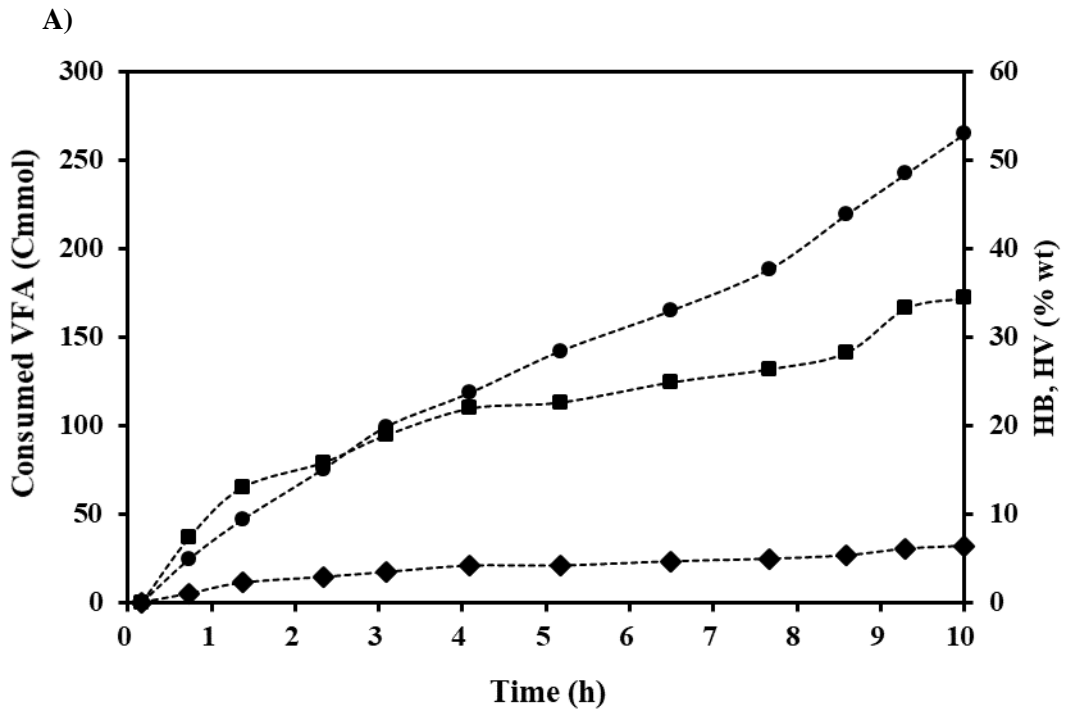
12

Figure 3

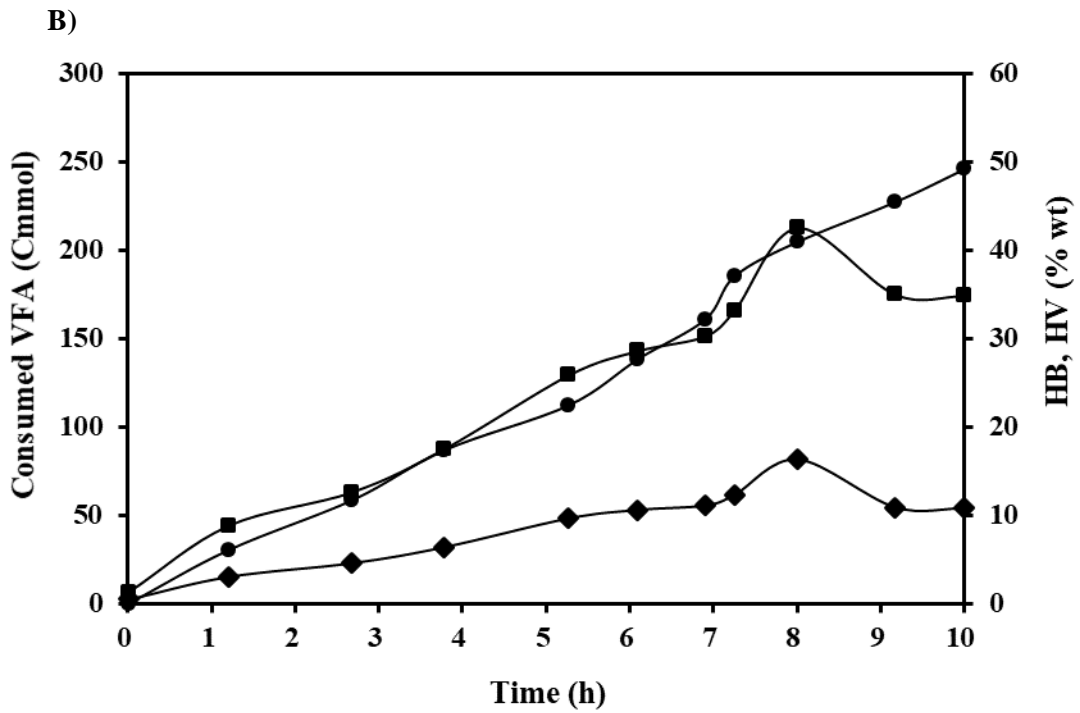


15

Figure 4



16



17

18

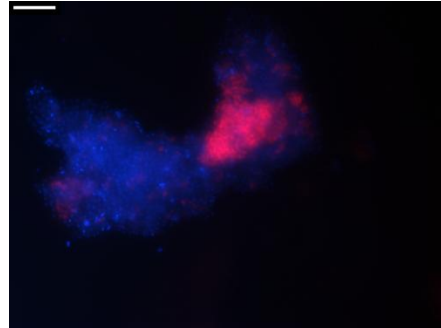
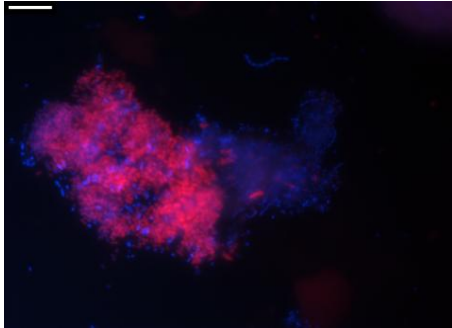
19

20 **Figure 5**

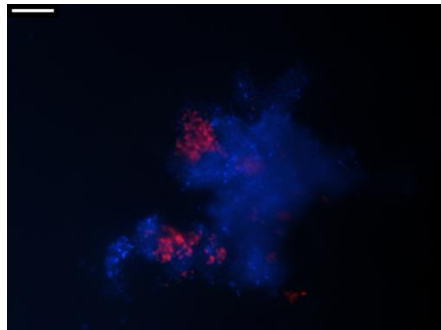
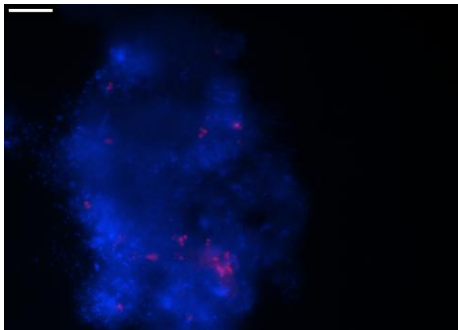
Inoculum from SBR-I

SBR-S on day 63

A



B



21

22

1 **FIGURE CAPTIONS**

2 **Figure 1.** Evolution in the SBR-S operational period of: A) the feast phase length (x)
3 and B) the VSS concentrations inside the SBR-S at the end of the cycle (the same as in
4 the effluent) at min 705 (○) and in the supernatant discharged after the settling stage (◆)
5 at min 200.

6 **Figure 2.** Evolution of the parameters monitored in representative enrichment cycles:
7 DO (-), VFA (●), X (■) and percentage of PHA accumulated (wt%) (▲). A) Reactor
8 operated without settling stage (SBR-I, - - -) at the moment of inoculum collection. B)
9 Reactor operated with settling stage (SBR-S, —) at day 62 of operation.

10 **Figure 3.** Proteins A), carbohydrates B) and TN C) concentrations before settling (*)
11 and after refilling (■) in the SBR-S reactor.

12 **Figure 4.** Evolution of the parameters monitored in accumulation essays (FBR)
13 performed with enriched biomass: VFA (●) and percentage of accumulated PHB (■)
14 and PHV (◆). A) Reactor operated without settling stage (FBR-I, - - -) at the moment of
15 inoculum collection. B) Reactor operated with settling stage (FBR-S, —) at day 64.

16 **Figure 5.** FISH images of the enriched biomass from the SBR-I (inoculum of SBR-S)
17 and SBR-S at day 63. A) *Comamonas* (Cte: Cy3, red) and all DNA (DAPI, blue) and B)
18 *Paraccocus* (Par1244; Cy3, red) and all DNA (DAPI, blue). The bar represents 10 μm.

Supplementary Material

[Click here to download Supplementary Material: Supplementary Material.doc](#)

*Declaration of Interest Statement

- 1 Declaration of interest none.

Credit Author Statement

Lucia Argiz: Investigation, Writing – Original Draft, Visualization; **Andrea Fra-Vazquez:** Conceptualization, Validation; **Angeles Val del Rio:** Validation, Visualization, Supervision, Funding Acquisition; **Anuska Mosquera:** Validation, Supervision, Project Administration, Funding Acquisition.